Modeling and validation of autoinducer-mediated bacterial gene expression in microfluidic environments

Caitlin M. Austin, William Stoy, Peter Su, Marie C. Harber, J. Patrick Bardill, Brian K. Hammer, and Craig R. Forest

Citation: Biomicrofluidics **8**, 034116 (2014); doi: 10.1063/1.4884519
View online: http://dx.doi.org/10.1063/1.4884519
View Table of Contents: http://scitation.aip.org/content/aip/journal/bmf/8/3?ver=pdfcov
Published by the AIP Publishing

Modeling and validation of autoinducer-mediated bacterial gene expression in microfluidic environments

Caitlin M. Austin,[1] William Stoy,[2] Peter Su,[3] Marie C. Harber,[1]
J. Patrick Bardill,[4] Brian K. Hammer,[4] and Craig R. Forest[1]
[1]*George W. Woodruff School of Mechanical Engineering, Georgia Institute of Technology, Atlanta, Georgia 30332, USA*
[2]*Wallace H. Coulter Department of Biomedical Engineering, Georgia Institute of Technology, Atlanta, Georgia 30332, USA*
[3]*Department of Chemical and Biomolecular Engineering, University of California, Berkeley, California 94720, USA*
[4]*School of Biology, Georgia Institute of Technology, Atlanta, Georgia 30332, USA*

(Received 11 April 2014; accepted 10 June 2014; published online 17 June 2014)

Biosensors exploiting communication within genetically engineered bacteria are becoming increasingly important for monitoring environmental changes. Currently, there are a variety of mathematical models for understanding and predicting how genetically engineered bacteria respond to molecular stimuli in these environments, but as sensors have miniaturized towards microfluidics and are subjected to complex time-varying inputs, the shortcomings of these models have become apparent. The effects of microfluidic environments such as low oxygen concentration, increased biofilm encapsulation, diffusion limited molecular distribution, and higher population densities strongly affect rate constants for gene expression not accounted for in previous models. We report a mathematical model that accurately predicts the biological response of the autoinducer N-acyl homoserine lactone-mediated green fluorescent protein expression in reporter bacteria in microfluidic environments by accommodating these rate constants. This generalized mass action model considers a chain of biomolecular events from input autoinducer chemical to fluorescent protein expression through a series of six chemical species. We have validated this model against experimental data from our own apparatus as well as prior published experimental results. Results indicate accurate prediction of dynamics (e.g., 14% peak time error from a pulse input) and with reduced mean-squared error with pulse or step inputs for a range of concentrations (10 μM–30 μM). This model can help advance the design of genetically engineered bacteria sensors and molecular communication devices. [http://dx.doi.org/10.1063/1.4884519]

I. INTRODUCTION

Using synthetic biology to genetically engineer bacteria that is responsive to molecular cues has enabled a variety of sensing applications. For example, engineered bacteria have been used as toxicology biosensors to detect the presence of pollutants including metals,[1] arsenic pollution,[2] and to monitor membrane biofouling.[3] These sensors are typically housed in flasks, wells, or agar plates,[1–3] but miniaturization is becoming increasingly common and important because it enables one to minimize reagents and to have greater control over stimuli, population size, density, flow rate, temperature, and other factors. As noted by van der Meer, and Belkin, "owing to their small size, bacterial bioreporter cells are highly suitable for incorporation onto microengineered platforms, transforming such devices into whole-cell biosensors."[4] Additionally polydimethylsiloxane (PDMS) is emerging as the material of choice for the design and fabrication of three-dimensional microfluidic networks of bacterial-cell arrays.[4]

To understand and engineer bacteria for sensor applications, several groups have examined the response of engineered bacteria to stimuli, either in bulk culture or in a microfluidic environment.[4] Whitaker *et al.*[5] showed the effect of population density on the ability of bacteria to respond in microliter-scale volume wells. Further, the effects of flow on reporter bacteria have been examined in a microfluidic device.[6] Delivering a chemical stimulus to engineered bacteria in a microfluidic environment, while monitoring fluorescent response, was done previously by Groisman *et al.*[7] Communication between two bacterial populations over time has been examined through means of a micro-ratchet structure[8] and self-regulating populations that act as oscillators.[9,10]

A variety of models for chemical transduction that apply to genetically engineered bacteria sensors have been posed that rely on a combination of the Hill equation,[11] Michaelis–Menten equation,[12] and general mass action (GMA) equations.[13] The Hill equation quantifies the degree of co-operativity of the binding of a ligand (e.g., N-Acyl homoserine lactone (AHL)) to a receptor (e.g., LuxR). In particular, the Hill coefficient in the Hill equation describes the fraction of the receptor saturated by ligand as a function of the ligand concentration. The Michaelis–Menten equation is one of the best known models of enzyme kinetics that relates reaction velocity to substrate concentration for a system where a substrate binds reversibly to an enzyme, forming a complex. GMA equations describe the dynamics of chemical species arising from reactions with kinetic rates. The rate of a chemical reaction is directly proportional to the molecular concentrations of the reacting species. Thus, a series of mass balances consisting of first-order differential equations can capture the dynamics between several chemical species that ultimately activate production of fluorescence (e.g., green fluorescent protein (GFP)).

Leveau and Lindow[14] made great strides towards modeling bacteria response by considering the activity of a promoter sequence as well as GFP maturation time and GFP degradation using such methods as Michaelis–Menten and a system of ordinary differential equations similar to GMA. This model has been utilized by many[15,16] for non-microfluidic environments. Since Leveau and Lindow's work, numerous attempts have been made to create a simplified model for reporter bacteria utilizing ordinary differential equations, the Hill equation or Michaelis–Menten equation. Previously, a series of ordinary differential equations was derived for the quorum sensing signaling pathway in *Vibrio fischeri* or *V. fischeri*.[17] Michaelis–Menten have been used to model the quorum sensing regulatory system of the *Aeromonas hydrophila*.[16] Another group looked to characterize a promoter with different number of DNA copies; with induction curves fitted with the Hill equation.[15] The use of this model is challenging because the necessary Hill coefficient varies widely between reports,[15,18] depends on specifics of the experimental system, and different forms of the Hill equation are often used as well. Both works were done in non-microfluidic settings.

In a previous study, the response of reporter bacteria to AHL was examined in microfluidic channels under flow and no-flow (quasi-static) conditions.[6] The Hill equation was used to predict the change in fluorescence over time using the input AHL concentration. Although the model included factors such as GFP degradation, the authors noted that "influences of a reduced oxygen concentration due to respiration, which might affect both the maturation of GFP and the cell physiology, were assumed to be negligible." This assumption, together with the over simplification of combining several chemical species and processes into a single equation, is limiting. In fact, the microfluidic environment, with time-varying inputs, exacerbates some of the shortcomings not only of the simplified models but also the more encompassing and general Leveau and Lindow model. This can lead to a poor fit between model and experimental data in microfluidic biological sensor literature.[6]

Microfluidic environments affect bacterial populations most importantly by limiting molecular distribution to diffusion. Under shear stresses prevalent in microfluidic environments with constant flow, biofilm formation is increased relative to wells or flasks with low shear stress flow or no flow.[19] Additionally *Escherichia coli*, or *E. coli*, commonly used for genetically engineered sensors, increase biofilm production in stressful environments[20] (i.e., low oxygen). Biofilm material slows diffusion of small molecules[21–23] such as oxygen and AHL. PDMS, a silicone elastomer often used for manufacturing microfluidic biosensors, is permeable to

oxygen, yet the oxygen concentration in a PDMS microfluidic biosensor can be considered diffusion limited, in contrast with open wells or flasks.[24] The concentration of oxygen in a PDMS microfluidic biosensor is difficult to predict, but it is influenced by geometry, especially, thickness to the external atmosphere, and the concentration of silicone elastomer to curing agent, which controls stiffness. Ultimately, oxygen concentration to the bacterial populations is influenced by biofilm, PDMS, atmospheric concentration, and oxygen dissolved in media. The expression of over 200 genes in *E. coli* can be affected by oxygen concentration,[25] and during the maturation of GFP, from immature GFP_i to mature GFP_m, a high amount of oxygen is needed.[26] The oxidation processes has been quantified and found to be rate limiting[27] and this has been quantified.[28]

We present a model that accounts for diffusion-limiting microfluidic environmental effects with experimental data collected from our microfluidic chambers, the design of which have been described previously.[29] The model utilizes a series of generalized mass action equations to describe the change in the concentration of each chemical species. After comparing this model and experiment, we apply the model to experimental data from Meyer *et al.*[6] to show its broad applicability.

II. METHODS

A. Bacteria

One of the common organisms used for biosensing is a genetically modified strain of *E. coli,* which expresses genes from the quorum sensing, or autoinducer, system of *V. fischeri*.[4] In *V. fischeri,* the lactone AHL reversibly binds to the regulatory LuxR protein. This complex then binds to the promoter for the *luxI* gene, inducing transcription. In genetically modified *E. coli*, the *luxI* promoter is engineered to control production of an unstable variant of GFP, thus, causing the bacteria to emit green fluorescence in the presence of AHL. The *E. coli* bacteria do not encode the genes to produce AHL, and thus act only as reporters.

To create a model for the sequence of biological processes, in which a population of genetically engineered reporter bacteria emits fluorescence in response to AHL stimulus, we first diagrammed the sequence of events that occur. Figure 1 shows a block diagram of the processes that occur in biosensing in *E. coli* with this LuxR system. Although this diagram is still a simplification of the signaling pathway from the literature,[30] it illustrates reactions and chemical species not accounted for in previous modeling efforts and is generally applicable for both macro- and microfluidic environments.

In this system, "external" AHL_e diffuses through the biofilm material surrounding the bacteria and subsequently across the bacteria membrane, becoming "internal" AHL_i at rate k_c. A constitutive promoter, P_{on}, drives the expression of the *luxR* gene that codes for the AHL receptor protein, LuxR at rate k_{Lc}. AHL_i and LuxR form a dimer complex (C_1), which reversibly binds to the *luxI* promoter sequence, P_{Lux}, forming complex C_2, which induces transcription and translation at rate k_{tr} of an unstable, immature variant of GFP_i. GFP_i folds into a mature fluorescent form GFP_m. Both GFP_i and GFP_m can degrade at rates k_{Gd} (see Figure 1).

We have previously reported our experimental methods but briefly summarize them here.[29] We used the microfluidic chip design of Danino *et al.*[9] to study our genetically engineered bacteria biosensors. This microfluidic design comprises a simple chamber for the bacteria population with an adjacent flow channel for delivery of both nutrients and chemical stimulus (AHL). This microfluidic environment facilitates control of stimulus concentration, stimulus duration, bacteria population size, temperature, flow rates, and measurement of response using fluorescence microscopy.

Standard microbiological techniques were used for culturing *E. coli*. All experiments were performed in 2xYT lysogeny broth (LB) media.[31] *E. coli* strain DH5α was used for all cloning. Reporter bacteria were derived from the fully sequenced K-12 strain MG1655.[32] To generate the reporter plasmid, Biobrick BBa T9002 (partsregistry.org) was modified using PCR based methods to append an ssrA-degradation tag (ANDENYALAA) to the C-terminus of GFP.[33] The resulting plasmid was transformed into MG1655 to create the reporter bacteria. Thus, the

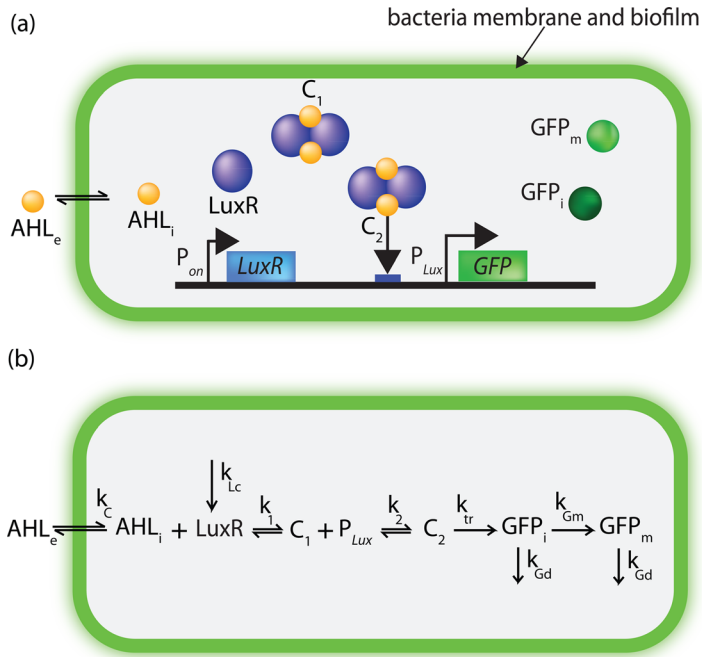

FIG. 1. (a) The genetically engineered *E. coli* strain MG1655 has a LuxR signaling pathway that receives external AHL (AHL_e) and produces mature GFP (GFP_m). (b) In this signaling pathway, we illustrate the most significant biological molecules (e.g., AHL_i and LuxR), complexes (denoted as C_n, where n is an integer), and gene sequences (e.g., promoter P_{Lux}) with rates, k_i.

E. coli strain MG1655 exhibits fluorescence upon receiving a specific AHL signal molecule, C6-HSL, as depicted in Figure 1.

B. Experimental setup

To fabricate the microfluidic devices, we utilized standard soft lithography[34] resulting in a PDMS device bonded to a glass coverslip. A PDMS central flow channel (250 μm wide $\times$ 10 μm high) is in direct fluidic contact with an adjacent PDMS chamber containing bacteria (100 μm $\times$ 100 μm $\times$ 5 μm high). Fluorescence was imaged on an upright microscope (Nikon TE 2000), through the glass coverslip with stage heated to 30 °C.

Bacteria were initially injected into the device through an inlet port using a syringe (BD, Luer-Lok), filling the chip entirely. Excess bacteria were flushed from the channel, leaving bacterial populations in the chambers. Bacteria were allowed to populate the chambers for 24 h to reach capacity ($\sim 10^5$), while the chamber was supplied with LB at 100 μl/h.

Once the bacteria had filled the chamber and biofilm had formed protecting the colony from shear stress, flow rate was increased to 360 μl/h. One syringe was used for LB (at 350 μl/h), while the second (10 μl/h) was used to deliver varying concentrations of AHL. A range of AHL concentrations exceeding prior published reports[5–7] was used to produce fluorescent responses up to saturation (0–30 μM). An "AHL pulse" is the duration and concentration over which this AHL was delivered to the bacteria chamber. Pulse durations of 50 min which we have previously optimized[29] were used. Fluorescent images were captured once in every 10 min and post-processed using MATLAB. The intensity of the pixels within the bacteria chamber was averaged and the background fluorescence was subtracted, yielding relative fluorescence (arbitrary units (AU)).

Three relative fluorescence levels are notable: a "threshold fluorescence" at 5% of peak, 95% of peak, and peak. A variety of durations were determined from the fluorescence responses measured and modeled. "Response delay" is defined as the time between the start of the AHL pulse and the time of threshold fluorescence. "Ramp-up time" is defined as the time between

the threshold fluorescence and 95% of peak. "Peak time" is defined as the time between the start of the AHL pulse and the time of peak fluorescence. "Response duration" is the duration that the response is above the threshold fluorescence. "Ramp-down time" is the time between the 95% of peak after achieving peak and threshold fluorescence. We computed the absolute value of the difference between measured and modeled durations at each concentration and averaged them. To ensure that outlier responses did not skew our data, we excluded any responses whose maximum amplitude were more than two standard deviations from the average. Experimental duration for setup, growth, and one cycle of stimulation and response averaged approximately two days.

C. Modeling

Our modeling method utilizes generalized mass action equations, GMA, based upon the chemical pathway shown in Figure 1(b). Transcription and translation were represented as a single species to simplify the model, while other biological processes affected by the microfluidic environment, such as diffusion of signal molecule AHL and maturation of GFP, were kept accessible. The general form of a GMA system of ordinary differential equations is given by

$$\dot{X}_i = \sum\left(\pm k_i \prod X_j\right), \tag{1}$$

where $\dot{X}_i$ is the rate of change of a concentration of molecular species i, k_i is the corresponding rate constant, and X_j is a concentration of molecular species j. For the processes described in Figure 1, the following equations were determined to model the bacteria response

$$\frac{dAHL_i}{dt} = k_c(AHL_e - AHL_i) - k_1 AHL_i^2 LuxR^2 + k_1 C_1, \tag{2}$$

$$\frac{dC_1}{dt} = k_1 AHL_i^2 LuxR^2 - k_1 C_1 + k_2 C_1 P_{Lux}, \tag{3}$$

$$\frac{dC_2}{dt} = k_2 C_1 P_{Lux} - k_2 C_2 - k_{tr} C_2, \tag{4}$$

$$\frac{dLuxR}{dt} = k_{Lc} - 2C_1 - 2C_2, \tag{5}$$

$$\frac{dGFP_i}{dt} = k_{tr} C_2 - k_{Gm} GFP_i - k_{Gd} GFP_i, \text{ and} \tag{6}$$

$$\frac{dGFP_m}{dt} = k_{Gm} G_i - k_{Gd} GFP_m. \tag{7}$$

AHL_i and AHL_e are the concentrations of internal and external AHL, respectively; LuxR is the population of free LuxR; C_1 is the LuxR-AHL dimer; C_2 is the complex involving the dimer bound to the promoter sequence; GFP_i represents "immature" GFP, in its inactive, non-fluorescent form; and GFP_m represents mature, fully fluorescent GFP.

The rate constant k_c governs mass transfer through the bacteria membrane and biofilm. Nilsson *et al.*[35] previously determined this rate of diffusion for membrane and biofilm separately; k_1 governs the association and dissociation of C_1; k_2 governs the association and dissociation of C_2; k_{Lc} represents the constitutive rate of production of LuxR; k_{tr} is the rate of protein production of GFP, encompassing transcription and translation; k_{Gm} governs GFP maturation; and k_{Gd} governs the rate of GFP degradation. Note that k_{Gd} is the same for both G_i and G_m, as GFP degradation proteases do not differentiate between the species. The vector **k** represents the set of rate constants $\mathbf{k} = [k_c\ k_1\ k_2\ k_{Lc}\ k_{tr}\ k_{Gm}\ k_{Gd}]$.

This system of ordinary differential equations was solved numerically in MATLAB using Euler's method. The set of initial values for the rate constants was based on literature as shown

TABLE I. Published and best-fit modeled rate constants for the metabolic processes for AHL-mediated GFP expression in reporter bacteria in a microfluidic environment. Sources for published bulk (non-microfludic) rates are noted and whether these published values were adjusted in our model to accommodate for the changes due to the microfluidic environment.

Rate constant	Rate description	Published bulk rate (h^{-1})	Best-fit microfluidic rate (h^{-1})	Adjusted	Source(s)
k_c	AHL diffusion	3600	254	Yes	35
k_1	C_1 formation/dissociation	60	60	No	17
k_2	C_2 formation/dissociation	600	600	No	17
k_{Lc}	LuxR production	1200	1200	No	39
k_{tr}	Protein production	150	1334	Yes	17
k_{Gm}	GFP maturation	3.6	1.8	Yes	17
k_{Gd}	GFP degradation	4.15	39	Yes	18

in Table I. Rate constants, k_1, k_2, and k_{Lc} were held fixed because they are processes that are independent of environment (e.g., oxygen concentration, biofilm) and thus literature values were assumed accurate, while k_c, k_{tr}, k_{Gm}, and k_{Gd} were allowed to vary by up to one order of magnitude from literature values. To determine the quality of fit for each vector **k**, the sum of square errors (SSE) was calculated between the numerically approximated result and the experimentally measured fluorescence. SSE was minimized by iteratively adjusting **k** with an interior-point algorithm.[36] After a set of rate constants that minimized SSE was found, their sensitivity was analyzed. Rate constants k_i were individually varied in increments of $\pm 100\%$, $\pm 10\%$, $\pm 1\%$, $\pm 0.1\%$, while holding the others constant to create a vector $\mathbf{k}_n$ for which a new SSE was calculated. The difference in error between **k** and $\mathbf{k}_n$ was then plotted to determine the sensitivity of each rate constant. This showed which variables have the greatest influence on the model and therefore must be considered when adjusting for the microfluidic environment.

III. RESULTS AND DISCUSSION

Figure 2 shows the relative fluorescence response of the bacterial populations in the microfluidic chambers to AHL stimuli of varying concentrations at constant 50 min duration. Figure 2 inset shows the amplitude of the relative fluorescence response to a 50 min pulse of AHL at concentrations from 10 μM to 30 μM (though 10 μM AHL did not elicit a response

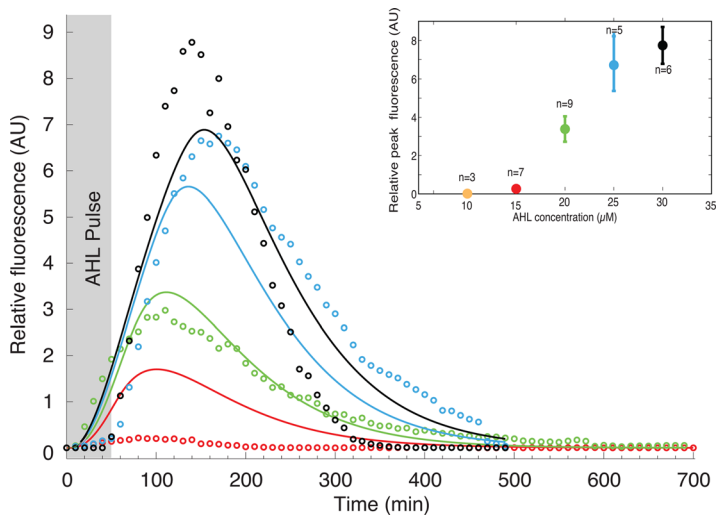

FIG. 2. Modeled response (lines) overlaid with measured experimental data for the linear regime of AHL concentrations. All used a 50 min pulse of AHL (indicated by shaded area) and varying concentrations (inset). Inset shows peak amplitude of the averaged fluorescence response as a function of AHL concentration with standard deviation and number of trials.

above the noise threshold (signal-to-noise ration greater than five[29]) and 30 μM approaches saturation). The relative fluorescence response data in Figure 2 is averaged across at least five trials at each concentration. For each concentration, experimentally and modeled, we determined threshold fluorescence, 95% of peak fluorescence, peak fluorescence, response delay, ramp-up time, response duration, and ramp-down time. Peak time averages 124.9 min for this range of concentrations. We measured an average absolute difference between the modeled and measured peak times for all concentrations as 17.1 min, or 14% error. Individually, peak time averages (and absolute differences between modeled and measured) were as follows: 79.8 min (22.6 min), or 28%, for 15 μM; 109.9 min (0.1 min), or 0%, for 20 μM; 170.0 min (32.8 min), or 19%, for 25 μM; and 140.0 min (12.9 min), or 9%, for 30 μM. To our knowledge, no other reported model for genetically engineered bacteria has the capability of predicting response peak time for time-varying stimuli. This feature of our model is important for applications in biosensing because the delay between stimulus and peak critically informs stimulus onset time.

Applications of engineered bacteria also involve communication networks,[29] in which the response delay, ramp-up time, response duration, and ramp-down time are important for data rate determination. Across all concentrations, we measured average (and absolute difference between modeled and measured) values as the following: response delay = 34.3 min (17.6 min), ramp-up time = 77.5 min (15.2 min), response duration = 344.5 min (114.5 min), and ramp-down times = 241.4 min (95.4 min). Corresponding errors range from 20% to 52%. These errors are large, but represent the first modeling effort to date at capturing such dynamics of a bacterial population in a microfluidic environment. Communication schemes are being developed[29,37,38] that accommodate these errors, while further efforts are underway to improve repeatability (see inset) and modeling accuracy. Experimental data collection are painstaking, and thus this data represent a sampling of the linear regime over which this bacterial system operates.

Parameter sensitivity analysis was conducted to determine the rate constants with the greatest effect on the model fit. Rate constants of high sensitivity produced divergent SSE values. The GMA model had the highest sensitivity to the rate parameter for GFP maturation, k_{Gm}. This shows the importance of adjusting this term to account for changes in the environment. Critically, during maturation of GFP, from immature GFP_i to mature GFP_m, a high amount of oxygen is needed[26] and thus this term is very sensitive to the microfluidic environment.

For the constant flow rate in all experiments, shear stress is constant, thus biofilm thickness is constant, and thus oxygen diffusion rate is constant. We verified that by lowering the AHL diffusion rate, k_c, the modeled bacterial response was slowed as expected.

Using parameter estimation, rate constants matching the kinetics of our system were determined, as shown in Table I (and used to generate the models of Figure 2). As previously mentioned, rate constants, k_1, k_2, and k_{Lc} are constant regardless of environmental factors (e.g., diffusion rate and oxygen concentration). AHL diffusion rate, k_c, was slowed from 3600 h^{-1} to 254 h^{-1}, a 93% change. This change accommodates dramatically slowed diffusion through the biofilm in addition to the bacteria membrane.

The GFP maturation rate, k_{Gm}, was decreased from 3.6 h^{-1} to 1.8 h^{-1}, a 50% change. This change has been suggested qualitatively in literature,[26] but has not heretofore been quantified for a microfluidic environment. Constant k_{Gm} is rate-limiting,[27] and our analysis confirms its sensitivity. Although it is not clear how the microfluidic environment can affect protein production rate (k_{tr}) and GFP degradation (k_{Gd}) rate, we note an increase in both in our model. Specifically, k_{tr} was found to increase by from 150 h^{-1} to 1334 h^{-1}. Some literature suggests that gene expression (e.g., k_{tr}) in *E. coli* can be affected by oxygen concentration,[25] but this is not well understood and indicates an area of future study. In our model, rate constant k_{Gd} was found to increase by nearly 10× over published values.[18] GFP degradation is not commonly studied since most prior work focuses on constant rather than time-varying inputs. Some have assumed changes in k_{Gd} are negligible,[6] and some have ignored this parameter altogether,[5] while we report here that it is critical and varies between the macro- and micro- environment.

The generalizability of this model to other microfluidic experiments with genetically engineered bacteria can be seen by examining the work done by Meyer *et al.*[6] In their study, a similar microfluidic environment was used to predict relative fluorescence of GFP by *Pseudomonas*

pupida IsoF biosensor strain in response to several external AHL concentrations, utilizing the Hill equation. To explore if our model was relevant to Meyer's data, we performed the following procedure. The published bulk rate values cited by Meyer were used to constrain our parameter estimation (see Meyer *et al.*[6] Table I). As before, rate constants k_1, k_2, and k_{Lc} were fixed, while k_c, k_{tr}, k_{Gm}, and k_{Gd} were allowed to vary by up to one order of magnitude from initial values with parameter estimation using the same Eqs. (2)–(7) and again minimizing SSE by iteratively adjusting **k** with an interior-point algorithm.

In Figure 3, we present a comparison of Meyer's model to our GMA model. Meyer acknowledged that their model did not fully describe the shape of the kinetics for this bacteria population.[6] As shown in Figure 3, our model better captures the shape of the response at later times by accommodating rate constants that capture reduced oxygen concentration. Both the Hill model and our generalized mass action model are first order responses to Meyer's step input, while the measured response exhibits second order dynamics. The Hill model better captures early dynamics (e.g., 0–240 min), while the error over the entire time period is greatly improved with our model. The models were quantitatively compared by calculating mean squared error (MSE) between each model fit and the data from Meyer. The MSE for the Meyer model fit was 1.62×10^6 AU, where our GMA model MSE was 1.28×10^4 AU, a two order of magnitude improvement.

We also explored the effect of different chamber widths (100 μm, 150 μm, 200 μm). Bacteria were allowed to populate the chambers for 24 h to reach capacity while the chambers were supplied with LB at 100 μl/h as before. Pulse durations of 50 min at 10 μM were used to elicit fluorescent responses. Ten chambers of each size were measured. A student t-test and Bayesian statistical methods were used to compare them. We found no statistical differences between the different sized chambers having equal density of bacteria.

Additionally, we also explored whether AHL degradation, due to bacteria consumption, should be included in the model. We found this effect was negligible, effectively zero, relative to the AHL mass transfer by diffusion through the bacteria membrane and biofilm (rate constant k_c).

We considered whether our results could be confounded by the temporal and spatial AHL gradients in the chamber. Both COMSOL Multiphysics modeling and experimental testing with Alexafluor 488-labeled BSA were used to verify that the time for the AHL to reach steady-state in the chamber was less than 3 s (at identical flow rate and temperature). At steady-state, the spatial concentration gradient across the chamber was less than 1%. Thus, both the temporal

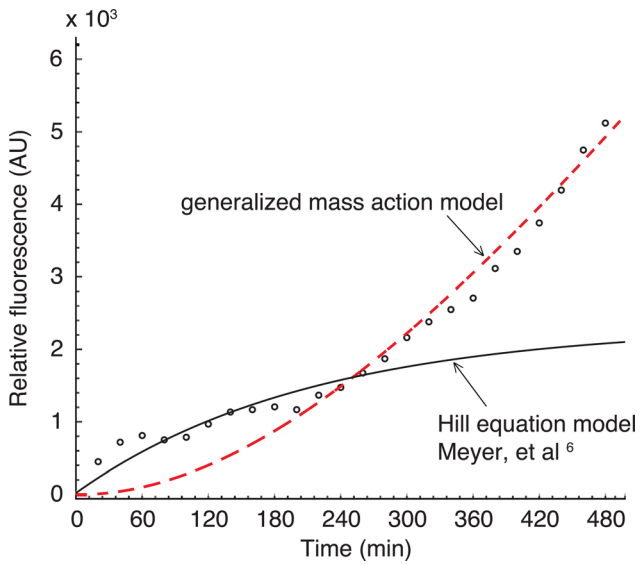

FIG. 3. Data (circles) and model (solid line) reproduced by permission from A. Meyer *et al.*, "Dynamics of AHL mediated quorum sensing under flow and non-flow conditions," Phys. Biol. **9**(2), 026007 (2012). Copyright 2012 IOP Publishing, Ltd. The generalized mass action model fit (dashed line) has an improved mean squared error over the duration of the experiment.

and spatial gradients are negligible relative to the bacteria fluorescent response. Similarly, the bacterial fluorescence response exhibited a spatial gradient in the chamber, which we measured by comparing the intensity of chamber sub-sections comprising of 50 000 bacteria. We found that the total intensity variation across the chamber to be negligibly less than 1%.

IV. CONCLUSION

Using a series of generalized mass action equations, we created a model that captures the dynamics of autoinducer-mediated bacterial gene expression, specifically AHL-mediated GFP expression, in reporter bacteria in a microfluidic environment. We subsequently fit that model to experimental data from both our laboratory and that of Meyer *et al.*[6] The model accurately captures the response peak time, with 14% error, and somewhat captures the response delay, ramp-up time, response duration, and ramp-down time for time-varying inputs across a range of input concentrations. The model is a substantial improvement, as measured by mean squared error, over previously reported models for time-constant inputs in microfluidic environments.

Four of the seven rate constants involved in metabolic processes for AHL-mediated GFP expression in reporter bacteria were found to vary between the macro-environment and the micro-environment explored in this work. By relaxing assumptions made in prior modeling efforts, we were able to capture AHL diffusion rate changes, GFP transcription and translation rate changes, GFP maturation rate changes, and GFP degradation rate changes. These rates changed due to increased biofilm formation in the microfluidic environment, which resulted in changes in oxygen and AHL concentration from what would be expected in bulk conditions. Most sensitively, GFP maturation is a sensitive, rate-limiting step, and this rate is greatly affected by oxygen content.

This model is versatile: applicable to microfluidic or traditional macro-environments; it can be used with time varying (pulse) or constant (step) inputs. This model can serve as a valuable tool in understanding genetically engineered bacteria and improving biosensor design capabilities, opening the door for sensors that adapt to environmental dynamics and communicate with each other.

ACKNOWLEDGMENTS

C.R.F., B.K.H., and J.P.B. are grateful for funding by the National Science Foundation (CISE 1110947). C.R.F. acknowledges funding by the National Science Foundation (EHR 0965945), NIH Single Cell Grant 1 R01 EY023173, NIH Computational Neuroscience Training Grant (DA032466-02), Georgia Tech Translational Research Institute for Biomedical Engineering & Science (TRIBES) Seed Grant Awards Program, Georgia Tech Fund for Innovation in Research and Education (GT-FIRE), Wallace H. Coulter Translational/Clinical Research Grant Program and support from Georgia Tech through the Institute for Bioengineering and Biosciences Junior Faculty Award, Technology Fee Fund, Invention Studio, and the George W. Woodruff School of Mechanical Engineering. C.M.A. and W.S. acknowledge the National Science Foundation Graduate Fellowship Program, without which this work would not be possible. P.S. is grateful for the National Science Foundation's National Nanotechnology Infrastructure Network (NNIN) Summer Research Experience for Undergraduates (REU) program that funded his participation in this research, and M.H. is thankful for the Georgia Tech President's Undergraduate Research Award and Undergraduate Research Opportunities Program that supported her contributions.

The authors declare no competing financial interest or conflict of interest in this work.

[1]T. Charrier *et al.*, "A multi-channel bioluminescent bacterial biosensor for the on-line detection of metals and toxicity. Part II: Technical development and proof of concept of the biosensor," Anal. Bioanal. Chem. **400**(4), 1061–1070 (2011).
[2]J. Stocker *et al.*, "Development of a set of simple bacterial biosensors for quantitative and rapid measurements of arsenite and arsenate in potable water," Environ. Sci. Technol. **37**(20), 4743–4750 (2003).
[3]M. F. Siddiqui *et al.*, "Targeting N-acyl-homoserine-lactones to mitigate membrane biofouling based on quorum sensing using a biofouling reducer," J. Biotechnol. **161**(3), 190–197 (2012).
[4]J. R. van der Meer and S. Belkin, "Where microbiology meets microengineering: Design and applications of reporter bacteria," Nat. Rev. Microbiol. **8**(7), 511–522 (2010).

[5]R. D. Whitaker *et al.*, "Single cell time-resolved quorum responses reveal dependence on cell density and configuration," J. Biol. Chem. **286**(24), 21623–21632 (2011).
[6]A. Meyer *et al.*, "Dynamics of AHL mediated quorum sensing under flow and non-flow conditions," Phys. Biol. **9**(2), 026007 (2012).
[7]A. Groisman *et al.*, "A microfluidic chemostat for experiments with bacterial and yeast cells," Nat. Methods **2**(9), 685–689 (2005).
[8]S. Park *et al.*, "Microfabricated ratchet structure integrated concentrator arrays for synthetic bacterial cell-to-cell communication assays," Lab Chip **12**(20), 3914–3922 (2012).
[9]T. Danino *et al.*, "A synchronized quorum of genetic clocks," Nature **463**(7279), 326–330 (2010).
[10]A. Prindle *et al.*, "A sensing array of radically coupled genetic 'biopixels'," Nature **481**(7379), 39–44 (2012).
[11]A. V. Hill, "The mode of action of nicotine and curari, determined by the form of the contraction curve and the method of temperature coefficients," J. Physiol. **39**(5), 361–373 (1909).
[12]L. Michaelis and M. M. Menten, "The kinetics of invertin action," FEBS Lett. **587**(17), 2712–2720 (2013).
[13]F. Horn and R. Jackson, "General mass action kinetics," Arch. Ration. Mech. Anal. **47**(2), 81 (1972).
[14]J. H. Leveau and S. E. Lindow, "Predictive and interpretive simulation of green fluorescent protein expression in reporter bacteria," J. Bacteriol. **183**(23), 6752–6762 (2001).
[15]S. Zucca *et al.*, "Characterization of an inducible promoter in different DNA copy number conditions," BMC Bioinf. **13**(Suppl 4), S11 (2012).
[16]C. Garde *et al.*, "Quorum sensing regulation in *Aeromonas hydrophila*," J. Mol. Biol. **396**(4), 849–857 (2010).
[17]M. Weber and J. Buceta, "Dynamics of the quorum sensing switch: Stochastic and non-stationary effects," BMC Syst. Biol. **7**, 6 (2013).
[18]S. Basu *et al.*, "A synthetic multicellular system for programmed pattern formation," Nature **434**(7037), 1130–1134 (2005).
[19]A. Park *et al.*, "Effect of shear stress on the formation of bacterial biofilm in a microfluidic channel," BioChip J. **5**(3), 236–241 (2011).
[20]H. L. Vieira, P. Freire, and C. M. Arraiano, "Effect of *Escherichia coli* morphogene bolA on biofilms," Appl. Environ. Microbiol. **70**(9), 5682–5684 (2004).
[21]P. S. Stewart, "Diffusion in biofilms," J. Bacteriol. **185**(5), 1485–1491 (2003).
[22]J. R. Lawrence, G. M. Wolfaardt, and D. R. Korber, "Determination of diffusion-coefficients in biofilms by confocal laser microscopy," Appl. Environ. Microbiol. **60**(4), 1166–1173 (1994).
[23]J. D. Bryers and F. Drummond, "Local macromolecule diffusion coefficients in structurally non-uniform bacterial biofilms using fluorescence recovery after photobleaching (FRAP)," Biotechnol. Bioeng. **60**(4), 462–473 (1998).
[24]S. G. Charati and S. A. Stern, "Diffusion of gases in silicone polymers: Molecular dynamics simulations," Macromolecules **31**(16), 5529–5535 (1998).
[25]M. Losen *et al.*, "Effect of oxygen limitation and medium composition on *Escherichia coli* fermentation in shake-flask cultures," Biotechnol. Progr. **20**(4), 1062–1068 (2004).
[26]R. Y. Tsien, "The green fluorescent protein," Annu. Rev. Biochem. **67**, 509–544 (1998).
[27]T. D. Craggs, "Green fluorescent protein: Structure, folding, and chromophore maturation," Chem. Soc. Rev. **38**(10), 2865–2875 (2009).
[28]R. Iizuka, M. Yamagishi-Shirasaki, and T. Funatsu, "Kinetic study of de novo chromophore maturation of fluorescent proteins," Anal. Biochem. **414**(2), 173–178 (2011).
[29]B. Krishnaswamy *et al.*, "Time-elapse communication: Bacterial communication on a microfluidic chip," IEEE Trans. Commun. **61**(12), 5139–5151 (2013); B. Krishnaswamy *et al.*, "When bacteria talk: Time elapse communication for super-slow networks," in *2013 IEEE International Conference on Communications (ICC)* (IEEE, 2013).
[30]P. V. Dunlap, "Quorum regulation of luminescence in *Vibrio fischeri*," J. Mol. Microbiol. Biotechnol. **1**(1), 5–12 (1999).
[31]L. Chong, "Molecular cloning - A laboratory manual, 3rd edition," Science **292**(5516), 446–446 (2001).
[32]F. R. Blattner *et al.*, "The complete genome sequence of *Escherichia coli* K-12," Science **277**(5331), 1453 (1997).
[33]J. B. Andersen *et al.*, "New unstable variants of green fluorescent protein for studies of transient gene expression in bacteria," Appl. Environ. Microbiol. **64**(6), 2240–2246 (1998).
[34]J. C. McDonald *et al.*, "Fabrication of microfluidic systems in poly(dimethylsiloxane)," Electrophoresis **21**(1), 27–40 (2000).
[35]P. Nilsson *et al.*, "Kinetics of the AHL regulatory system in a model biofilm system: How many bacteria constitute a 'quorum'?," J. Mol. Biol. **309**(3), 631–640 (2001).
[36]R. H. Byrd, M. E. Hribar, and J. Nocedal, "An interior point algorithm for large-scale nonlinear programming," SIAM J. Optim. **9**(4), 877–900 (1999).
[37]I. F. Akyildiz *et al.*, "Monaco: Fundamentals of molecular nano-communication networks," IEEE Wireless Commun. **19**(5), 12–18 (2012).
[38]M. Pierobon and I. F. Akyildiz, "Capacity of a diffusion-based molecular communication system with channel memory and molecular noise," IEEE Trans. Inf. Theory **59**(2), 942–954 (2013).
[39]Y. Tanouchi *et al.*, "Noise reduction by diffusional dissipation in a minimal quorum sensing motif," PLoS Comput. Biol. **4**(8), e1000167 (2008).